OPEN

Stainless steel bipolar plate coated with polyaniline/Zn-Porphyrin composites coatings for proton exchange membrane fuel cell

M. A. Deyab [1*] & G. Mele[2]

The proton exchange membrane fuel cells are the promising sustainable energy sources. The present study focuses on the enhancement the fuel cell performance and the protection of the stainless steel bipolar plate from the corrosion using polyaniline/Zn-Porphyrin composites coatings. The electrochemical properties (polarization and impedance) of the coated 303 stainless steel in 1.0 M H_2SO_4 solution have been evaluated. The coated 303 stainless steel by new composites exhibits the excellent anti-corrosion activity towards corrosive fuel cell electrolyte. The polyaniline/Zn-Porphyrin composite gives an excellent performance by adding 1.0% of Zn-Porphyrin. This composite improves the output power of the fuel cell.

Proton-exchange membrane fuel cells (PEMFC) create power by changing over chemical energy (hydrogen and oxygen gas) to electrical power. Because of the high cost of PEMFC components, the usage of this cell is limited[1]. The bipolar plates are the one of the main components in fuel cell. It works as conductor for electrical current from cell to cell[2]. The graphite is the foremost commonly utilized material for bipolar plates manufacture[3]. It has many advantages such as the great corrosion resistance. On another hand, there are many problems facing the use of graphite as the bipolar plates such as its brittle texture and high gas permeability[4]. The use of metallic materials for constructing bipolar plates has been highly welcomed in scientific circles[5–7]. They characterize by high electrical conductivity and low cost. Most commercialized bipolar plates made nowadays are stainless steel[8]. Metal corrosion is a huge problem, particularly in bipolar plates[9]. The presence of corrosion products and passive layer on the bipolar plate's surface decrease the performance of PEMFC. To address this problem, many scientists have developed different conductive coatings to screen the metallic bipolar plates[10–12]. These coatings prevent the bipolar plate's corrosion and consequently improve the PEMFC performance. Researchers have taken a major step towards protect the bipolar plates using conductive polymer coatings such as polyaniline (PANI)[13]. This kind of polymers is characterized by good conductivity and high thermal stability[14]. To maximize the efficiency of PANI, the combination of carbon nanotubes (CNT) with PANI was developed by many researchers[15]. Ramezanzadeh[16] proposed polyaniline modified GO nanosheets coatings to improve the performance of stainless steel bipolar plate. Sharma and his colleagues[17] improved the corrosion Resistance stainless steel bipolar plates using composite PANI and titanium nitride nanoparticle. Jiang et al.[18] investigated the graphene oxide incorporated polypyrrole(PPY) matrix. The results showed that PPY-GO composite coatings work as good anti-corrosion coatings for stainless steel bipolar plates in the aggressive solutions. Gao et al.[19] reported phosphomolybdic acid doped PANI coating for corrosion protection of 303SS. Show and his colleagues[20] used CNT/PTFE composite coating for stainless steel bipolar plate. This coating decreased the contact resistance and increased the output power of the fuel cell. Here, we prepared a new composite coating for stainless steel bipolar plate. The base of this composite coating is polyaniline polymer (PANI) with Zn-Porphyrin (Zn-Pr). The main functions of new composite are the increasing the corrosion resistance of stainless steel bipolar plate and the enhancing output power of the fuel cell. The porphyrin molecules have very attractive properties. Its structure defined as a group of heterocyclic macrocycle organic compounds[21]. The insert of metals like Zn, Ni, and Co into porphyrin macrocycle structure influence on the optical absorption spectrum and the electrical and magnetic properties[21]. To our knowledge, this is the first study to use PANI/Zn-Pr composites coatings for PEMFC.

[1]Egyptian Petroleum Research Institute (EPRI), PO Box 11727, Nasr City, Cairo, Egypt. [2]Department of Engineering for Innovation of University of Salento, via Arnesano, 73100, Lecce, Italy. *email: hamadadeiab@yahoo.com
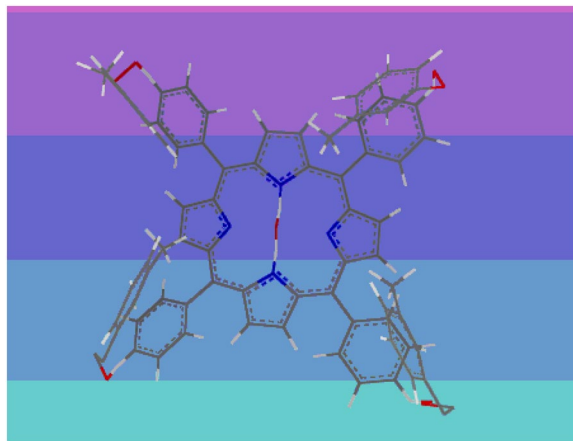
Figure 1. Zn-Porphyrin structure.

Experimental

Materials.   Grade 303 stainless steel (303SS) (composition %: 0.15 C; 2.0 Mn; 1.0 Si; 0.2 P; 0.15 S; 17 Cr; 8 Ni; balance Fe) was used as the bipolar plate. The 303SS was cut into rectangle shape specimens with total surface area 1.12 cm^2. These specimens were cleaned according to standard methods ASTM G1–03.

Polyaniline polymer and sulfuric acid (98%) were supplied from SigmaeAldrich Co. Xylene was supplied from PRABHAT CHEMICALS Co.

Zn-Porphyrin (Fig. 1) was synthesized according to the reported procedure[22].

PANI/Zn-Pr composites preparation and application of coating.   The xylene (10 ml) and Zn-Pr powder (0.5, 0.8 and 1.0 gm) were mixed using mechanical stirrer (part 1). The xylene and PANI (1:1 ratio) (90 ml) were mixed using a high speed mechanical stirrer (part 2). The final composite was obtained by mixing part 1 and part 2 using mechanical stirrer followed by ultrasonication (3.0 h) and then ground for 1.0 h to obtain the desired fineness. PANI/Zn-Pr composites coatings were applied on the whole surface of clean 303SS using spray gun (Walther PILOT). The coated 303SS samples were cured at 343 K for 1.0 h.

The dry thickness of the PANI and PANI/Zn-Pr composites films was in the range 53 ± 5 μm using Elcometer 456 gauge (Elcometer Co).

Permeability Testing Cups (BYK Instruments) offer a simple method to check the permeability of PANI/Zn-Pr composites coatings within a 24 h period.

Electrochemical measurements.   The anti-corrosion of new PANI/Zn-Pr composite coating was evaluated using potentiodynamic polarization and electrochemical impedance spectroscopy (EIS) techniques.

The polarization curves were recorded using recommended scan rate (1.25 mV s^{-1}) in the potential range ± 250 mV with regard to the open circuit potential.

EIS plots were recoded in the the frequency range 0.01 Hz–100 kHz at the open circuit potential. The AC voltage amplitude was 10 mV. Electrochemical data were collected using Potentiostat/Galvanostat (model Gill AC, 947, ACM).

The electrochemical experiments were repeated at least 3 times to ensure accuracy. All values are presented in the form of mean values and standard deviation.

PEMFC performance measurements.   For the PEMFC performance test, the laboratory single cell fuel cell testing stations from Fuel Cell Store was used. In this cell, H_2 and O_2 gas were flow with rate 150 ml/min. Bare 303SS and coated 303SS were used as bipolar plates. Nafion 117 was used as the proton electrolyte membrane. Platinum particles on acetylene black powder (as support) were used as the catalyst on the surface of anode and cathode electrodes.

Results and Discussion

Anti-corrosion performance of PANI/Zn-Pr composites.   We first recoded the polarization responses of uncoated stainless steel bipolar plate 303SS in 1.0 M H_2SO_4 solution. The same experiments were applied for coated 303SS by neat PANI and PANI/Zn-Pr composites. All these curves are collected in Fig. 2.

The corrosion potential (E_{corr}) and corrosion current density (j_{corr}) were extracted form Tafel curves[23] (see Table 1) to assess anti-corrosion performance of PANI/Zn-Pr composites.

The j_{corr} values of coated 303SS by neat PANI and PANI/Zn-Pr composites were much lowers than that of the control 303SS. The incorporation of Zn-Pr molecules into PANI leads to increase its anti-corrosion performance. This is clearly shown through the considerable decrease of j_{corr} values form 5.90 μA cm^{-2} to 0.15 μA cm^{-2}. It was noted also there is a significant shift in E_{corr} to more noble direction in the cases of PANI/Zn-Pr composites, indicating the protective effect of new composites[24]. Here, the composites layer covered both cathodic and anodic sites on the surface of 303 SS and caused the shifting in the E_{corr} values.

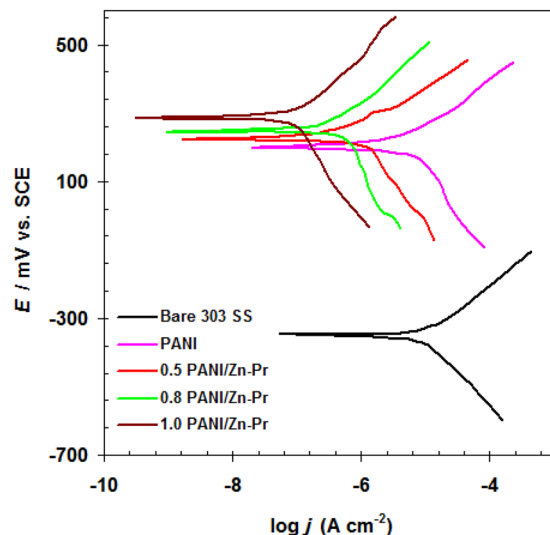We calculated anti-corrosion efficiencies (η_j%) of coatings from the Eq. (1)[25].

Figure 2. Polarization curves of uncoated and coated 303SS by neat PANI and PANI/Zn-Pr composites in 1.0 M H_2SO_4 solution at 298 K.

Sample	j_{corr} (µA cm^{-2})	E_{corr} mV vs. SCE	η_j %
Bare 303SS	25.68 ± 1.05	-347 ± 5.7	—
PANI	5.90 ± 0.45	193 ± 3.8	77.02
0.5% PANI/Zn-Pr	1.24 ± 0.23	221 ± 4.3	95.17
0.8% PANI/Zn-Pr	0.39 ± 0.04	224 ± 4.8	98.48
1.0% PANI/Zn-Pr	0.15 ± 0.02	284 ± 5.1	99.41

Table 1. Electrochemical parameters and the corresponding corrosion inhibition efficiency for uncoated and coated 303 SS in 1.0 M H_2SO_4 solution at 298 K.

Sample	H_2O permeability cm^2 s^{-1}
PANI	1.36×10^{-6}
0.5% PANI/Zn-Pr	2.55×10^{-7}
1.0% PANI/Zn-Pr	9.03×10^{-8}

Table 2. Water permeability of PANI coating in the absence and presence of Zn-Pr at 298 K.

$$\eta_j\% = \frac{j^o_{corr} - j^c_{corr}}{j^o_{corr}} \times 100 \tag{1}$$

where j^o_{corr} and j^c_{corr} are the corrosion rates for uncoated and coated 303 SS, respectively.

In the case of coated samples with neat PANI, the η_j% was 77.02% (see Table 1). The use of PANI/Zn-Pr composites leads to enhance the anti-corrosion efficiency of PANI. The maximum efficiency was obtained at 1.0% of Zn-Pr (Table 1).

The permeability of composites coatings is an important property to measure the electrolyte transfer through a coatings film. The presence of pores across the PANI coating is responsible for allowing corrosive cell electrolyte permeation. Therefore, blocking these pores can result in effectively hindering the corrosion of bipolar plates. In this respect, the dispersion of Zn-Pr particles in the texture of PANI coating leads to low electrolyte permeability of the PANI/Zn-Pr composites compared to neat PANI coating (see Table 2).

Electrochemical impedance spectroscopy. To exclude the effect of anti-corrosion and conductivity activities caused by the addition of Zn-Pr, we measured the electrochemical impedance responses (Nyquist plot) of bare 303SS, neat PANI and PANI/Zn-Pr composites in 1.0 M H_2SO_4 solution. All measurements were achieved after 7 days.

We found that the Nyquist plots for bare 303SS comprise of two capacitive loops (see Fig. 3). The best an equivalent circuit described this case is given in Fig. 4.

The electrolyte resistance was represented by R_s. The passive film resistance and capacitance were represented by R_f and C_f, respectively. R_{ct} and C_{dl} are charge transfer resistance and double layer capacitor related to 303SS/
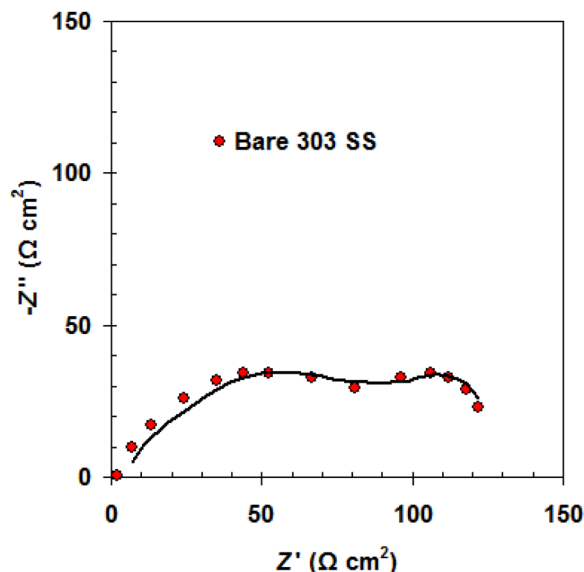
Figure 3. Nyquist plot of bare 303 SS in 1.0 M H_2SO_4 solution at 298 K.
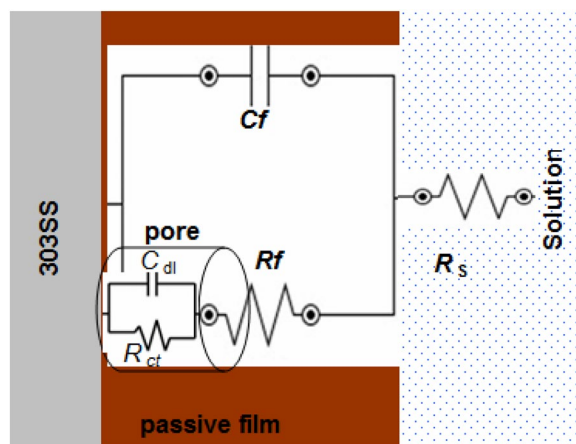

Figure 4. Equivalent circuit to fit the impedance bare 303 SS in 1.0 M H_2SO_4 solution.

H_2SO_4 solution interface[26]. We noted that the Nyquist plots for coated samples by the neat PANI and PANI/Zn-Pr composites were changed to one capacitive loop (at high frequencies) and straight line (at low frequencies) (Fig. 5)[27]. This line is due to diffusion impedance of the coating barrier layer (Z_d)[28]. The equivalent circuit described, the PANI and PANI/Zn-Pr composites (0.5% Zn-Pr) is shown in Fig. 6. In this case, C_c and R_c represent the capacitance and resistance of the coating layer, respectively.

By incorporation 1.0% of Zn-Pr into PANI coating, the Z_d part for diffusion process was disappeared and the equivalent circuit was represented only by C_c and R_c elements (see Fig. 7).

All the equivalent circuit elements for uncoated and coated samples are listed in Tables 3 and 4.

Initially the R_c value of PANI coatings is comparatively low than for passive film R_f. This implies that the PANI coatings have considerable conductivity if it compares with the passive layer formed on the bare 303SS[18,29]. By incorporation Zn-Pr into PANI coating, the coating resistance R_c increased and the coating capacitance C_C decreased.

Here, Zn-Pr particles repair the PANI coating flaws and block the passage of corrosive solution towards 303 SS substrate and caused the changing in the R_c and C_C values.

This indicates that Zn-Pr plays a vital role in enhancing the anti-corrosion property of PANI coatings. Furthermore, at 1.0% of Zn-Pr, the PANI coating become a very good barrier for restriction the diffusion of corrosive solution.

PEMFC performance. To assess the effect of the PANI/Zn-Pr composites coating on the PEMFC Performance, we explored the reliance of the current density on the output cell voltage and the power density for single PEMFC cell using uncoated or coated 303SS bipolar plates. This data was showed in Fig. 8(a,b).
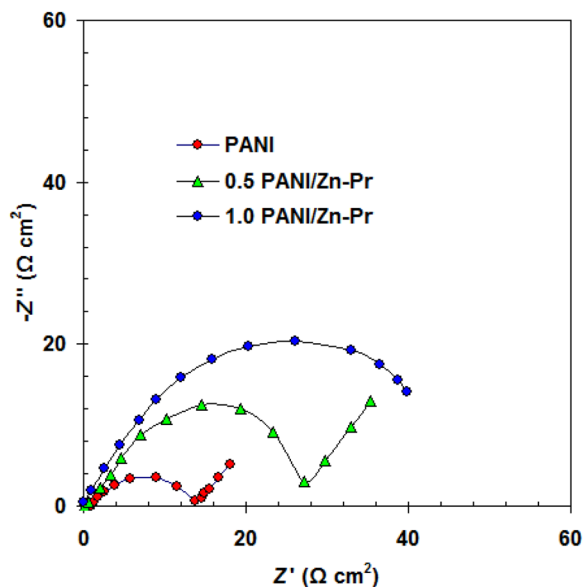
Figure 5. Nyquist plots for coated 303 SS by the neat PANI and PANI/Zn-Pr composites in $1.0\,M\,H_2SO_4$ solution at 298 K.
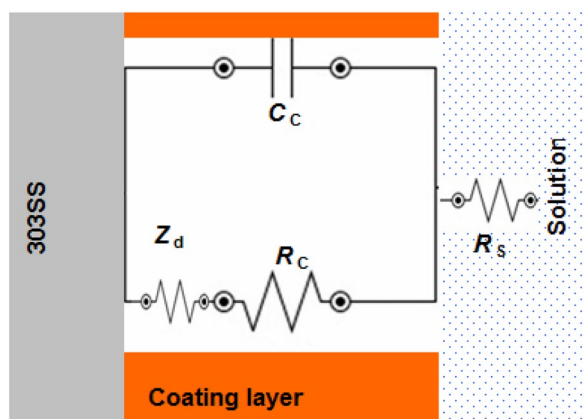

Figure 6. Equivalent circuit to fit the impedance coated 303 SS by the neat PANI and PANI/Zn-Pr composite (0.5% Zn-Pr) in $1.0\,M\,H_2SO_4$ solution.
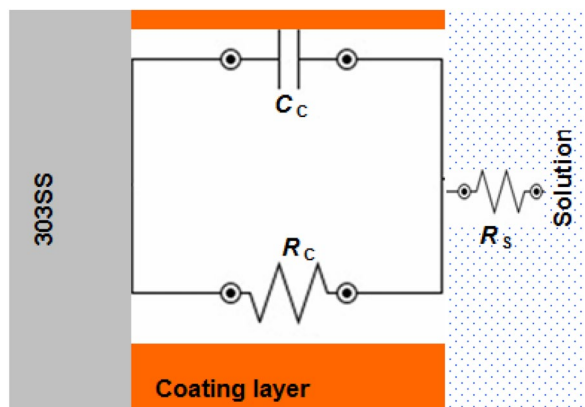

Figure 7. Equivalent circuit to fit the impedance coated 303 SS by PANI/Zn-Pr composite (1.0% Zn-Pr) in $1.0\,M\,H_2SO_4$ solution.

Sample	$R_f\,\Omega\,cm^2$	$C_f\,\mu F\,cm^{-2}$	$R_{ct}\,\Omega\,cm^2$	$C_{dl}\,\mu F\,cm^{-2}$
Bare 303 SS	76.40 ± 2.3	204 ± 4.7	55.65 ± 1.3	193 ± 2.6

Table 3. Fitted electrochemical parameters of 303 SS in 1.0 M H_2SO_4 solution at 298 K.

Sample	$R_c\,\Omega\,cm^2$	$C_c\,\mu F\,cm^{-2}$	$Z_d\,\Omega\,cm^2$
PANI	13.6 ± 1.2	398 ± 3.5	6.8 ± 0.3
0.5% PANI/Zn-Pr	26.8 ± 1.3	234 ± 4.6	14.6 ± 0.4
1.0% PANI/Zn-Pr	48.3 ± 1.6	212 ± 2.7	—

Table 4. Fitted electrochemical parameters of coated 303 SS in 1.0 M H_2SO_4 solution at 298 K.
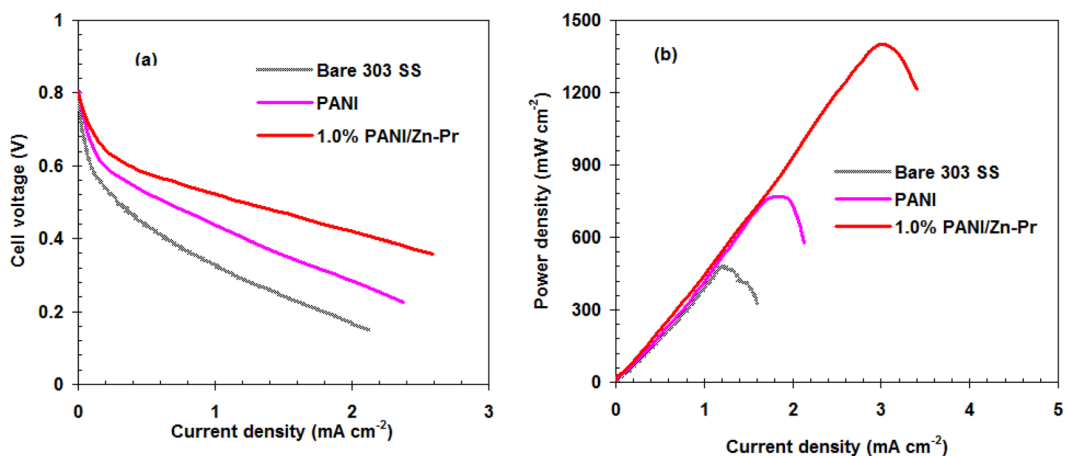
Figure 8. Output cell voltage (**a**) and power density (**b**) for single PEMFC cell using uncoated and coated 303 SS bipolar plates.

The open voltage for all samples was 0.805 V. Generally, the out voltage cell decreased with current density increasing due to IR drop[30]. The out voltage in the case of coated 303SS bipolar plates by PANI/Zn-Pr composites was significantly decreased comparing with bare bipolar plates and neat PANI bipolar plates (see Fig. 8(a)).

The supreme power density for single PEMFC cell using uncoated 303SS bipolar plates is 435 mW cm^{-2} (Fig. 8(b)). This value was increased to 720 and 1353 mW cm^{-2} in the case of neat PANI and PANI/Zn-Pr composite, respectively. This confirms that the using of PANI-Zn-Pr composite leads to increase the performance of PEMFC cell.

Mechanism and explanation. The above results reveal the strong effect of Zn-Pr on the anti-corrosion effect of PANI coating for 303SS bipolar plates, leading to an increased PEMFC performance.

The 303SS bipolar plates suffered from the corrosion and dissolution during the immersion in cell electrolyte. In addition, the passive film formed during the corrosion process, led to the increase in the contact resistance and the membrane electrodes contamination[31,32].

The PANI coating plays as a barrier for 303SS bipolar plates. Where this coating decreases the contact between the 303SS surface and corrosive electrolyte. But the performance of PANI coating is not high enough to prevent the bipolar plate's corrosion due to the presence of pores in the texture of PANI polymer[33]. These pores allow the passage of corrosive solution to contact with the bipolar plates[34]. The corrosive ions enhance the active dissolution of 303SS[35,36]. These ions may lead to pitting corrosion and induce metal failure[37].

The incorporation of Zn-Pr with PANI polymer to form PANI/Zn-Pr composite, leads to efficiency coating barrier. The main role of Zn-Pr is the reducing the pores in the PANI polymer texture[10,38]. This will significantly affect on the degree of contact between the 303SS surface and corrosive electrolyte.

Additionally, the presence of Zn-Pr molecules act as a conductive path though PANI polymer, leading to the increase in the output power of the PEMFC cell[39,40]. The conducting characterization of Zn-Pr molecules is due to the aromaticity of the macrocycle, leading to the electrons mobility though the PANI/Zn-Pr composite[41,42].

Conclusions

PANI/Zn-Pr composites coatings have been developed, which is effective to significantly increase the output power of the PEMFC cell and decrease the degree of contact between the 303SS bipolar plates and corrosive electrolyte. Anti-corrosion properties of PANI/Zn-Pr composites were confirmed using polarization experiments to define their anti-corrosion efficiency. The highest anti-corrosion activity of the PANI/Zn-Pr composite (i.e. 99.41%) was obtained at 1.0% of Zn-Pr. EIS data also further confirmed that the Zn-Pr plays a significant role

in enhancing the coating resistance of PANI. The use of coated 303SS bipolar plates by PANI/Zn-Pr composites leads to increase the output density for single PEMFC cell. Therefore, the new PANI/Zn-Pr composites are considered effective coatings for bipolar plates in future PEMFC technologies.

References

1. Napoli, R., Gandiglio, M., Lanzini, A. & Santarelli, M. Techno-economic analysis of PEMFC and SOFC micro-CHP fuel cell systems for the residential sector. *Energ. Buildings* **103**, 131–146 (2015).
2. Tawfik, H., Hung, Y. & Mahajan, D. Metal bipolar plates for PEM fuel cell—A review. *J. Power Sources* **163**, 755–767 (2007).
3. Jiang, L. *et al*. Design and testing criteria for bipolar plate materials for PEM fuel cell applications. *Mater. Res. Soc. Symp. Proc.* **393**, 151–155 (1995).
4. Mehta, V. & Cooper, J. S. Review and analysis of PEM fuel cell design and manufacturing. *J. Power Sources* **114**, 32–53 (2003).
5. Antunes, R. A., Oliveira, M. C. L., Ett, G. & Ett, V. Corrosion of metal bipolar plates for PEM fuel cells: A review. *Int. J. Hydrogen Energy* **35**, 3632–3647 (2010).
6. Karimi, S., Fraser, N., Roberts, B. & Foulkes, F. R. A Review of Metallic Bipolar Plates for Proton Exchange Membrane Fuel Cells: Materials and Fabrication Methods. *Adv. Mater. Sci. Eng.* **2012**, 1–22 (2012).
7. Yuan, X. Z., Wang, H., Zhang, J. & Wilkinson, D. P. Bipolar plates for PEM fuel cells-from materials to processing. *J. New Mater. Electrochem. Syst.* **8**, 257–267 (2005).
8. Kumagai, M., Myung, S.-T., Kuwata, S., Asaishi, R. & Yashiro, H. Corrosion behavior of austenitic stainless steels as a function of pH for use as bipolar plates in polymer electrolyte membrane fuel cells. *Electrochim. Acta* **53**, 4205–4212 (2008).
9. Jiang, L. *et al*. Electropolymerization of camphorsulfonic acid doped conductive polypyrrole anti-corrosive coating for 304SS bipolar plates. *Appl. Surf. Sci.* **426**, 87–98 (2017).
10. Deyab, M. A. Corrosion protection of aluminum bipolar plates with polyaniline coating containing carbon nanotubes in acidic medium inside the polymer electrolyte membrane fuel cell. *J. Power Sources* **268**, 50–55 (2014).
11. Kahveci, E. E. & Taymaz, I. Experimental study on performance evaluation of PEM fuel cell by coating bipolar plate with materials having different contact angle. *Fuel* **253**, 1274–1281 (2019).
12. Ren, Y. J. & Zeng, C. L. Effect of conducting composite polypyrrole/polyaniline coatings on the corrosion resistance of type 304 stainless steel for bipolar plates of proton-exchange membrane fuel cells. *J. Power Sources* **182**, 524–530 (2008).
13. Qiu, C., Liu, D., Jin, K., Fang, L. & Xie, G. J. Robertson, Electrochemical functionalization of 316 stainless steel with polyaniline-graphene oxide: Corrosion resistance study. *Mater. Chem. Phys.* **198**, 90–98 (2017).
14. Ho, W.-Y., Pan, H.-J., Chang, C.-L., Wang, D.-Y. & Hwang, J. Corrosion and electrical properties of multi-layered coatings on stainless steel for PEMFC bipolar plate applications. *Surf. Coatings Technol.* **202**, 1297–1301 (2007).
15. Luo, C., Xie, H., Wang, Q., Luo, G. & Liu, C. A Review of the Application and Performance of Carbon Nanotubes in Fuel Cells. *Journal of Nanomaterials*, **Article ID 560392**, 1–10 (2015).
16. Ramezanzadeh, B., Mohamadzadeh Moghadam, M. H., Shohani, N. & Mahdavian, M. Effects of highly crystalline and conductive polyaniline/graphene oxide composites on the corrosion protection performance of a zinc-rich epoxy coating. *Chem. Eng. J.* **320**, 363–375 (2017).
17. Sharma, S., Zhang, K., Gupta, G. & Santamaria, D. G. Exploring PANI-TiN Nanoparticle Coatings in a PEFC Environment: Enhancing Corrosion Resistance and Conductivity of Stainless Steel Bipolar Plates. *Energies* **10**, 1–13 (2017).
18. Jiang, L., Syed, J. A., Lu, H. & Meng, X. *In-situ* electrodeposition of conductive polypyrrole-graphene oxide composite coating for corrosion protection of 304SS bipolar plates. *J. Alloys Compd.* **770**, 35–47 (2019).
19. Gao, Y. Z., Syed, J. A., Lu, H. B. & Meng, X. K. Anti-corrosive performance of electropolymerized phosphomolybdic acid doped PANI coating on 304SS. *Appl. Surf. Sci.* **360**, 389–397 (2016).
20. Show, Y. & Takahashi, K. Stainless steel bipolar plate coated with carbon nanotube (CNT)/polytetrafluoroethylene (PTFE) composite film for proton exchange membrane fuel cell (PEMFC). *J. Power Sources* **190**, 322–325 (2009).
21. Kadish, W., Smith, K. M. & Guilard, R. Handbook of Porphyrin Science; World Scientific Publishing Co.: Singapore, Volume **44** (2016).
22. Deyab, M. A. *et al*. Synthesis and characteristics of alkyd resin/M-Porphyrins nanocomposite for corrosion protection application. *Prog. Org. Coat.* **105**, 286–290 (2017).
23. Deyab, M. A., Zaky, M. T. & Nessim, M. I. Inhibition of acid corrosion of carbon steel using four imidazolium tetrafluoroborates ionic liquids. *J. Mol. Liq.* **229**, 396–404 (2017).
24. Deyab, M. A. M. Corrosion Inhibition and Adsorption Behavior of Sodium Lauryl Ether Sulfate on L80 Carbon Steel in Acetic Acid Solution and Its Synergism with Ethanol. *J. Surfact. Deterg.* **18**, 405–411 (2015).
25. Deyab, M. A., Keera, S. T. & El Sabagh, S. M. Chlorhexidine digluconate as corrosion inhibitor for carbon steel dissolution in emulsified diesel fuel. *Corros. Sci.* **53**, 2592–2597 (2011).
26. Prajila, M., Rugmini Ammal, P. & Joseph, A. Comparative studies on the corrosion inhibition characteristics of three different triazine based Schiff's bases, HMMT, DHMMT and MHMMT, for mild steel exposed in sulfuric acid. *Egypt. J. Pet.* **27**, 467–475 (2018).
27. Deyab, M. A. Decyl glucoside as a corrosion inhibitor for Magnesium–air battery. *J. Power Sources* **325**, 98–103 (2016).
28. Wang, Y. *et al*. Preparation and performance of electrically conductive Nb-doped TiO_2/polyaniline bilayer coating for 316 L stainless steel bipolar plates of proton-exchange membrane fuel cells. *RSC Adv.* **8**, 19426–19431 (2018).
29. Moghadam, M. H. M., Sabury, S., Gudarzi, M. M. & Sharif, F. Graphene oxide-induced polymerization and crystallization to produce highly conductive polyaniline/graphene oxide composite. *J. Polym. Sci. Pol. Chem.* **52**, 1545–1554 (2014).
30. Zhang, J. PEM Fuel Cell Electrocatalysts and Catalyst Layer (Springer, London), pp. 359–361. (2008).
31. Deyab, M. A. Effect of halides ions on H_2 production during aluminum corrosion in formic acid and using some inorganic inhibitors to control hydrogen evolution. *J. Power Sources* **242**, 86–90 (2013).
32. Deyab, M. A. Hydrogen generation during the corrosion of carbon steel in crotonic acid and using some organic surfactants to control hydrogen evolution. *Int. J. Hydrog. Energy* **38**, 13519–13511 (2013).
33. Zhang, K. & Sharma, S. Site-Selective, Low-Loading, Au Nanoparticle–Polyaniline Hybrid Coatings with Enhanced Corrosion Resistance and Conductivity for Fuel Cells. *ACS Sustain. Chem. Eng.* **5**, 277–286 (2017).
34. Abaci, S. & Nessark, B. Characterization and corrosion protection properties of composite material (PANI + TiO_2) coatings on A304 stainless steel. *J. Coat. Technol. Res.* **12**, 107–120 (2015).
35. Deyab, M. A. Electrochemical investigations on pitting corrosion inhibition of mild steel by provitamin B5 in circulating cooling water. *Electrochim. Acta* **202**, 262–268 (2016).
36. Deyab, M. A., Essehli, R. & El Bali, B. Performance evaluation of phosphate $NaCo(H_2PO_3)3.H_2O$ as a corrosion inhibitor for aluminum in engine coolant solutions. *RSC Adv.* **5**, 48868–48874 (2015).

37. Foad El-Sherbini, E. E., Abd-El-Wahab, S. M., Amin, M. A. & Deyab, M. A. Electrochemical behavior of tin in sodium borate solutions and the effect of halide ions and some inorganic inhibitors. *Corros. Sci.* **48**, 1885–1898 (2006).
38. Deyab, M. A. Effect of carbon nano-tubes on the corrosion resistance of alkydcoating immersed in sodium chloride solution. *Prog. Org. Coat.* **85**, 146–150 (2015).
39. Deyab, M. A., De Riccardis, A. & Mele, G. Novel epoxy/metal phthalocyanines nanocomposite coatings for corrosion protection of carbon steel. *J. Mol. Liq.* **220**, 513–517 (2016).
40. Deyab, M. A., De Riccardis, A., Bloise, E. & Mele, G. Novel H2Pc/Epoxy nanocomposites: Electrochemical and mechanical property investigation as anti-corrosive coating. *Prog. Org. Coat.* **119**, 31–35 (2018).
41. Collman, J. P. *et al.* Conductive polymers derived from iron, ruthenium, and osmium metalloporphyrins: The shish-kebab approach. *Proc. Natl. Acad. Sci.* **83**, 4581–4585 (1986).
42. Collman, J. P. *et al.* Synthetic, electrochemical, optical, and conductivity studies of coordination polymers of iron, ruthenium, and osmium octaethylporphyrin. *J. Am. Chem. Soc.* **109**, 4606–4614 (1987).

Author contributions

Study concept, design analysis, interpretation of data, preparation the electrode, electrochemical experiments, wrote the main manuscript text by M.A. Deyab. Preparation of Zn-Porphyrin, material characterization analysis by G. Mele Critical review of manuscript for important intellectual content – All authors.

Competing interests

The authors declare no competing interests.

Additional information

Correspondence and requests for materials should be addressed to M.A.D.

Reprints and permissions information is available at www.nature.com/reprints.

Publisher's note Springer Nature remains neutral with regard to jurisdictional claims in published maps and institutional affiliations.